JOURNAL OF MATERIALS SCIENCE 30 (1995) 6083–6089

The assessment of particle friction of a drug substance and a drug carrier substance

F. PODCZECK, J. M. NEWTON
The School of Pharmacy, Department of Pharmaceutics, University of London, 29/39 Brunswick Square, London, WC1N 1AX, UK

M. B. JAMES
Glaxo Research & Development Ltd, Park Road, Ware, Hertfordshire, SG12 0DP, UK

The centrifuge technique, which has been previously used in adhesion experiments, has been modified for use in single particle friction studies. Both flat compacted surfaces and large single particles were used as substrate surfaces to allow assessment of drug–drug, drug–drug carrier and drug carrier–drug carrier friction forces. Particle size, particle shape and surface roughness were identified as main factors influencing the change from a static into a dynamic friction process and the division between friction due to adhesion and ploughing. The forces of adhesion and friction were found to be proportional to the reversible energy of adhesion. The ratio between the force of adhesion and the press-on force applied and the ratio between the force of friction and the press-on force can be related to the yield stress and the reduced Young's modulus of the materials in contact.

1. Introduction

Friction phenomena play a key role in handling of powders, such as powder flow, powder compression or lubrication. In the field of pharmaceutics, friction has been mainly studied on the bulk properties of a powder [1, 2]. Alternatively, compacts such as tablets have been used [3, 4] to study the phenomena. However, in the latter case the particle surface properties may not necessarily be reflected by the surface of the compacts. In powder aerosol preparations small drug particles are added to carrier particles to aid subdivision of the dose and administration to the patient. A balance of adhesion forces is necessary to achieve subdivision of the dose, yet allowing particle detachment of the respirable drug particles during inhalation. In addition to adhesion forces, friction between the drug carrier particles and the drug substance particles will be involved during the detachment process. A model to study single particle friction was first described by Zimon [5]. Using Zimon's approach, a value for the static friction force can be derived. An indirect method, i.e. the assessment of the force needed to clean a semiconductor surface, was described by Khilnani [6]. Here, the cleaning force depends on the angle between force vector and surface and the coefficient of friction. Measuring the necessary cleaning force at a given angle, the coefficient of friction could be calculated. Recently, Podczeck *et al.* [7] have reported an approach to measure the friction force of single particles on plastic surfaces adapting a centrifuge technique [8, 9] originally used in adhesion measurements.

The classical theory of friction [10] describes the friction force, F_{frict}, as a resultant force due to adhesion, F_{ad}, and ploughing, F_{Pl}

$$F_{frict} = F_{ad} + F_{Pl} \quad (1)$$

Sometimes a third mechanism, which is the friction due to deformation of asperities of the contacting surfaces, is added to Equation 1 [11–13]. However, the deformation of asperities and the adhesion are strongly related factors [14, 15], and a split of the adhesion term into an adhesion and a deformation term appears difficult.

Several physical properties of the surfaces in contact influence the friction force. Such factors are the surface roughness [16], the surface free energy [17, 18] and the plastic and/or elastic deformability of the surface asperities [19–21]. The relation between the adhesion and ploughing component of the friction force of particles sticking to surfaces depends on the relationship between the indentation hardness of the surface and the particles [22], and there is no general ratio evaluating the influence of the adhesion on friction against the ploughing component [23].

Friction forces are quoted only occasionally. Commonly, the coefficient of friction (the ratio between force of resistance to moving and normal load) is determined, and there are some laws linking the coefficient of friction to the physical properties of the surfaces in contact [17, 24, 25]. One way of calculating both a coefficient of friction and a friction force for particle friction on flat surfaces can be derived using the relationship described by Bhattacharya and Mittal [26]

$$\mu = \frac{F_{rem} \times \cos \alpha}{F_{ad} + F_{rem} \times \sin \alpha} \quad (2)$$

0022–2461

where F_{rem} is the removal force; F_{ad}, the force of adhesion; μ, the static coefficient of friction; and α, the angle between the removal force vector and the surface. To use this equation the force vector applied to remove the particles in an angled direction has to pass first the particle and then the surface. However, in the centrifuge technique [7] the force vector involved in the detachment of the particles form the surface in an angled direction, F_{det}, passes first the surface and then the particle. Therefore, the effective force to remove the particles from the surface is now the difference between F_{ad} and $F_{det} \times \sin\alpha$, and Equation 3 can be proposed

$$\mu = \frac{F_{det} \times \cos\alpha}{F_{ad} - F_{det} \times \sin\alpha} \quad (3)$$

This equation can be validated for the two extreme cases, which are $\alpha = 0°$ (friction) and $\alpha = 90°$ (adhesion) by rearrangement into Equation 4

$$F_{det} = \frac{\mu \times F_{ad}}{\cos\alpha + \mu \sin\alpha} \quad (4)$$

with $\alpha = 90°$

$$F_{det} = F_{ad} \quad (5)$$

and $\alpha = 0°$

$$F_{det} = \mu \times F_{ad} \quad (6)$$

Equations 5 and 6 are the classical definitions for adhesion and friction [10].

To estimate both the friction force and the static coefficient of friction, Equation 3 has to be rewritten into a linear function

$$F_{det} \times \cos\alpha = -\mu \times F_{det} \times \sin\alpha + \mu \times F_{ad} \quad (7)$$

The static coefficient of friction can be obtained from the slope of this function, whereas the friction force is the intercept with the ordinate ($\mu \times F_{ad}$).

The aim of this work was to assess single particle friction forces and coefficients of friction of powders, which are either attached to surfaces of identical material, or on surfaces made from a second powdered material. The single particles were both tested in particle-on-surface experiments, i.e. the powder particles sliding along a flat compacted powder surface, and in particle-on-particle experiments, i.e. the powder particles moving along the surface of larger carrier particles. Different particle size fractions were used to investigate the role of the contact area between the contiguous bodies. The resulting friction forces and coefficients of friction should be related to properties, such as surface roughness, reversible energy of adhesion and deformability of the materials in contact.

2. Experimental procedure

Two different particle size fractions of a drug substance, Salmeterol Xinafoate, and a drug carrier substance, lactose monohydrate, were investigated. The particle size fractions were prepared using an air jet sieve (Alpine, Augsburg, Germany). The average particle mass of each particle size fraction was determined by difference using an AD-4 Perkin Elmer autobalance. Samples were weighed onto a cover slip to give the mass, and then suspended in glycerol triacetate in the case of lactose, or in liquid paraffin in the case of Salmeterol Xinafoate. The number of particles per sample was counted automatically with a Seescan Solitaire 512 image analyser fitted with a black/white CCD-4 camera and an Olympus microscope. Each average particle mass is the mean of five replicated determinations. The number mean particle size of each particle size fraction (Feret's diameter [27]) was assessed by image analysis. Three suspended powder samples of each particle size fraction were investigated measuring 1000 particles on each occasion. Table I lists the results of the particle mass and particle size measurements.

TABLE I Characteristics of the particle size fractions of Salmeterol Xinafoate and lactose

Fraction	[a]m (ng)	[b]F (μm)
Lactose		
LF1	80.84 ± 3.89	62.3
LF2	215.05 ± 16.34	77.6
Salmeterol Xinafoate		
SFa	63.97 ± 8.18	35.9
SFb	384.27 ± 82.05	57.2

[a] m, particle mass ($\bar{x} \pm s$, $n = 5$).
[b] F, Feret's diameter.

Flat compacted powder surfaces were produced using an Instron, model TT, universal testing instrument. The resulting discs were 3 mm in height and had a diameter of 10 mm. For particle-on-particle experiments a special particle size fraction of lactose (which comprised particles of a size between 180 and 250 μm) was prepared by sieving.

The general outline of the centrifuge technique, including the details about the centrifuge cells used, is described by Podczeck *et al.* [7] and by Lam and Newton [9]. The centrifuge tubes were deposited into a fixed angle rotor head (60°) of a Fisons MSE High Speed 18 ultracentrifuge. For adhesion experiments the centrifuge tubes were placed into the rotor pockets, assuring that the substrate surfaces and the centrifugal force vector were 90° to each other. To achieve a friction process instead of an adhesion experiment, the centrifuge tubes had to be turned in their rotor pockets, so that substrate surface and centrifuge force vector resulted in an angle smaller than 90°. In this way, friction angles between 30 and 80° could be studied.

The preparation of centrifuge samples for particle-on-surface friction tests is similar to the preparation for adhesion studies, which is described in detail by Podczeck *et al.* [28]. Similarly, the preparation of the centrifuge samples for particle-on-particle experiments can be obtained from Podczeck *et al.* [29].

All samples had to undergo a preliminary "press-on" centrifugation, i.e. a centrifuge force was applied to increase the contact between particles and surface. In this case, the angle between surface and centrifugal

force vector was 90°, and the disc surfaces were directed to the rotor axis. The press-on speed was always 8000 r.p.m., from which equivalent forces can be calculated.

The initial amount of particles attached to the substrate surface and the amount of particles remained sticking to the surface after applying a detachment force was determined using the image analysis by manual counting. The sample surfaces were lit using an Olympus cold light source. The two light beams were positioned at an angle of 180° to each other, parallel to and at a distance of 1.5 cm from the perimeter of the substrate surface. The relative amount of particles remaining on the surface was treated as a function of the detachment force, from which a median detachment force and an interquartile range could be determined.

The surface roughness of the flat compacted powder surfaces was determined using a Talysurf 6 stylus profilometer instrument with a 2 μm stylus tip and 0.8 mm cut off. The average surface roughness, rugosity, is expressed as R_a, which is the arithmetic mean of the departures of the roughness profiles from the mean line. Three discs of each material were tested, and R_a was assessed from five random tracks across the surface of each disc. The R_a value for lactose surfaces is 2.01 ± 0.15 μm, and the R_a value for Salmeterol Xinafoate surfaces is 0.30 ± 0.02 μm.

3. Results and discussion

The lactose particles of either particle size fraction were tested in particle-on-surface experiments on flat lactose surfaces only. In accordance to the terminology used in adhesion [5], the process studied will be called "autofriction".

As reported previously [7], a decrease in the angle α between the flat surface and the centrifuge force vector leads firstly to an increase in the detachment force compared to the adhesion force determined at $\alpha = 90°$, but at lower angles of α a sudden drop in detachment force often occurs. This can be interpreted as a change from static friction into dynamic friction. Table II summarizes the results for the autofriction of lactose particles. The change from static autofriction into a dynamic autofriction occurs for particle size fraction LF1 between a friction angle α of 50–60°, whereas for LF2 the sliding and/or rolling of the particles starts below 50°, as can be seen from the drop in the detachment force values. The friction force (calculated from Equation 7) increases with the particle size tested, whereas the coefficient of friction (calculated from Equation 7) decreases. The increase in friction force with particle size might be due to a larger number of contact points between the two surfaces in contact, because the true contact area is proportional to the measured friction force [30]. The coefficient of friction should be a fixed material constant, but several authors have shown, that this value varies according to the external load applied [16, 19, 20]. Using the calculated coefficient of friction in Equation 6 to estimate the friction force due to adhesion, it appears as though adhesion is the only

TABLE II Results of the autofriction measurements on lactose particles autoadhered to flat compacted lactose surfaces ($x \pm s$, $n = 6$)

	[a]LF1	LF2
[b]F_{on} ($\times 10^{-9}$ N)	4.91	13.10
[c]F_{ad} ($\times 10^{-9}$ N)	1.25 ± 0.39	3.63 ± 2.38
	[f]$\alpha = 70°$	$\alpha = 70°$
[d]F_{det} ($\times 10^{-9}$ N)	1.45 ± 0.45	3.68 ± 1.00
[e]IQR ($\times 10^{-9}$ N)	1.80 ± 0.39	4.72 ± 0.80
	$\alpha = 60°$	$\alpha = 50°$
F_{det} ($\times 10^{-9}$ N)	2.87 ± 0.18	3.83 ± 0.78
IQR ($\times 10^{-9}$ N)	2.30 ± 0.29	4.07 ± 0.40
	$\alpha = 50°$	$\alpha = 40°$
F_{det} ($\times 10^{-9}$ N)	0.70 ± 0.13	2.50 ± 0.66
IQR ($\times 10^{-9}$ N)	0.78 ± 0.11	3.32 ± 0.44
	$\alpha = 30°$	$\alpha = 30°$
F_{det} ($\times 10^{-9}$ N)	0.69 ± 0.09	2.22 ± 1.15
IQR ($\times 10^{-9}$ N)	0.86 ± 0.10	2.91 ± 1.57
[g]F_{fric} ($\times 10^{-9}$ N)	0.26 ± 0.25	1.50 ± 0.19
[h]μ	0.41	0.32
$\mu \times F_{ad}$ ($\times 10^{-9}$ N)	0.51	1.16
[i]P ($\times 10^{-9}$ N)	–	0.34

[a] LF, lactose particle fraction.
[b] F_{on}, press-on force.
[c] F_{ad}, median force of autoadhesion.
[d] F_{det}, median detachment force.
[e] IQR, interquartile range.
[f] α, angle between centrifuge force vector and surface.
[g] F_{fric}, friction force.
[h] μ, coefficient of static friction.
[i] P, friction force due to ploughing.

mechanism involved in the friction of particles of the lactose fraction LF1 (see Table II), whereas particles of size fraction LF2 cause ploughing, although the adhesion term still dominates. (The ploughing force has been calculated using Equation 1.) The interquartile range of the detachment forces characterizes the differences in the detachment force necessary for the single particles of the assortment of particles sticking onto a surface. For lactose particles autoadhered to lactose surfaces the interquartile range increased with the increase in particle size form LF1 to LF2, and decreased with increased α, indicating that dynamic friction is less variable than static friction if the particle size of a narrow particle size fraction is studied.

Table III summarizes the autofriction results of Salmeterol Xinafoate on flat compacted Salmeterol Xinafoate surfaces. Static autofriction only occurs for large values of α (particle size fraction SFa: $\alpha \geq 80°$, particle size fraction SFb: $\alpha \geq 70°$). The exact angle, where static autofriction changes into dynamic autofriction could not be determined, but for particle size fraction SFa this change occurs between 80 and 70°, whereas for particle size fraction SFb the change is between 70 and 60°. The friction force and the coefficient of friction decrease with particle size. The two fractions of Salmeterol Xinafoate particles are very different in their morphology. Particles of size fraction SFa are irregular, but particles of size fraction SFb are spherical. Therefore, particles of size fraction SFb should have less contact points with the compact surface and therefore a smaller friction force

TABLE III Results of the autofriction measurements on Salmeterol Xinafoate particles autoadhered to flat compacted Salmeterol Xinafoate surfaces ($x \pm s$, $n = 6$)

	[a]SFa	SFb
[b]F_{on} ($\times 10^{-9}$ N)	3.89	4.99
[c]F_{ad} ($\times 10^{-9}$ N)	3.81 ± 0.09	0.72 ± 0.19
	[f]$\alpha = 80°$	$\alpha = 70°$
[d]F_{det} ($\times 10^{-9}$ N)	3.57 ± 0.33	1.21 ± 0.18
[e]IQR ($\times 10^{-9}$ N)	2.06 ± 0.21	1.46 ± 0.28
	$\alpha = 70°$	$\alpha = 60°$
[g]F_{det} ($\times 10^{-9}$ N)	2.47 ± 0.32	0.76 ± 0.16
IQR ($\times 10^{-9}$ N)	2.14 ± 0.16	1.12 ± 0.14
	$\alpha = 50°$	$\alpha = 50°$
F_{det} ($\times 10^{-9}$ N)	1.72 ± 0.17	0.61 ± 0.15
IQR ($\times 10^{-9}$ N)	1.99 ± 0.26	1.03 ± 0.20
	$\alpha = 30°$	$\alpha = 30°$
F_{det} ($\times 10^{-9}$ N)	1.04 ± 0.13	0.25 ± 0.51
IQR ($\times 10^{-9}$ N)	1.42 ± 0.17	0.41 ± 0.12
[g]F_{frict} ($\times 10^{-9}$ N)	1.38 ± 0.05	0.25 ± 0.06
[h]μ	0.22	0.18
$\mu \times F_{ad}$ ($\times 10^{-9}$ N)	0.84	0.13
[i]P ($\times 10^{-9}$ N)	0.54	0.12

[a] SF, Salmeterol Xinafoate particle fraction.
[b] F_{on}, press-on force.
[c] F_{ad}, median force of autoadhesion.
[d] F_{det}, median detachment force.
[e] IQR, interquartile range.
[f] α, angle between centrifuge force vector and surface.
[g] F_{frict}, friction force.
[h] μ, coefficient of static friction.
[i] P, friction force due to ploughing.

TABLE IV Results of the friction measurements on Salmeterol Xinafoate particles adhered to flat compacted lactose surfaces and lactose particles ($x \pm s$, $n = 6$)

	[a]SFa (on surface)	SFb (on surface)	SFa (on particle)
[b]F_{on} ($\times 10^{-9}$ N)	3.89	4.99	3.89
[c]F_{ad} ($\times 10^{-9}$ N)	1.97 ± 0.20	0.33 ± 0.14	1.03 ± 0.26
	[f]$\alpha = 70°$	$\alpha = 70°$	$\alpha = 70°$
[d]F_{det} ($\times 10^{-9}$ N)	1.49 ± 0.44	0.12 ± 0.04	1.95 ± 0.23
[e]IQR ($\times 10^{-9}$ N)	7.80 ± 0.73	0.18 ± 0.04	2.05 ± 0.36
	$\alpha = 50°$	$\alpha = 50°$	$\alpha = 60°$
F_{det} ($\times 10^{-9}$ N)	6.63 ± 0.77	0.34 ± 0.06	1.63 ± 0.13
IQR ($\times 10^{-9}$ N)	5.09 ± 0.82	0.45 ± 0.07	1.74 ± 0.12
	$\alpha = 40°$	$\alpha = 40°$	$\alpha = 50°$
F_{det} ($\times 10^{-9}$ N)	1.36 ± 0.18	0.88 ± 0.22	1.40 ± 0.18
IQR ($\times 10^{-9}$ N)	2.22 ± 0.31	1.60 ± 0.38	1.43 ± 0.07
	$\alpha = 30°$	$\alpha = 30°$	$\alpha = 30°$
F_{det} ($\times 10^{-9}$ N)	2.44 ± 0.81	0.12 ± 0.04	1.20 ± 0.09
IQR ($\times 10^{-9}$ N)	2.80 ± 0.53	1.83 ± 0.46	1.44 ± 0.16
[g]F_{frict} ($\times 10^{-9}$ N)	0.85 ± 0.55	–	1.24 ± 0.04
[h]μ	0.68	–	0.31
$\mu \times F_{ad}$ ($\times 10^{-9}$ N)	1.34	–	0.32
[i]P ($\times 10^{-9}$ N)	–	–	0.92

[a] SF, Salmeterol Xinafoate particle fraction.
[b] F_{on}, press-on force.
[c] F_{ad}, median force of adhesion.
[d] F_{det}, median detachment force.
[e] IQR, interquartile range.
[f] α, angle between centrifuge force vector and surface.
[g] F_{frict}, friction force.
[h] μ, coefficient of static friction.
[i] P, friction force due to ploughing.

is reasonable. Furthermore, spherical particles undergo only rolling friction, which should be expressed by a lower friction force. Both adhesion and ploughing appear to take part in the autofriction of Salmeterol Xinafoate particles, but adhesion still dominates the process in the case of particle size fraction SFa. In general, for Salmeterol Xinafoate the interquartile range is smaller for particle size fraction SFb than for particle size fraction SFa (see Table III). Rolling friction should depend mainly on the particle diameter, which has a narrow range for particles of one size fraction. Sliding friction should depend mainly on the true contact area between the particles attached and the surface, if adhesion was involved in the process. The true contact area of irregular particles, such as Salmeterol Xinafoate particle size fraction SFa, is far more variable, and therefore the detachment forces are also more variable.

In Table IV the results of the friction measurements of Salmeterol Xinafoate particles on flat compacted lactose surfaces are listed. The change from a static friction into a dynamic friction occurs between friction angles of 50–40° and 40–30° for particle size fractions SFa and SFb, respectively. These are far lower values than those for the autofriction of Salmeterol Xinafoate particles. The friction between particles of size fraction SFb and the lactose surfaces could not be described successfully. The coefficient of friction calculated was larger than 1.0, and the friction force was negative.

Therefore, only the results of autofriction and friction of particle size fraction SFa can be compared. The coefficient of friction is about three times larger for friction on lactose than for autofriction, and adhesion appears to be the only mechanism involved. The compacted surfaces of lactose and Salmeterol Xinafoate are different in their energetic properties, because Salmeterol Xinafoate has a lower surface free energy [29], and the lactose discs provide a rougher surface structure than Salmeterol Xinafoate discs (see Experimental procedure). A connection between surface roughness and the coefficient of friction is reported in the literature [31]. The results reported here suggest an increase in static friction with increased surface roughness. The asperities of the substrate surface are a kind of mechanical barrier, which must be overcome before the movement of the particles along the surface can occur.

Comparing the friction angles, at which the change between static and dynamic friction occurs, of all tests undertaken on flat compacted surfaces, it appears that the range of α is proportional to the particle size. For the large particle fractions SFb and LF2, the change always occurred 10° below the range of α found for the smaller particle size fractions SFa and LF1. Hence, the transformation between static and dynamic friction depends on the particle size. The larger the particles, the smaller is the friction angle, where first sliding or rolling processes occur.

Adhesion experiments using Salmeterol Xinafoate particle size fraction SFa and large lactose particles as carrier material had shown, that particle-on-particle

measurements lead to smaller adhesion forces than particle-on-surface experiments [29]. Hence, the following experiments have been undertaken to test whether this is also the case in friction force measurements. The results of the particle-on-particle friction experiments for Salmeterol Xinafoate particle size fraction SFa on lactose particles are also summarized in Table IV.

Static friction only occurs at a friction angle of $\geq 70°$. This is in contrast to the measurements on the flat compacted lactose surfaces. It can be explained, however, if the surface structure of the lactose particles is taken into account. The lactose particles provide a surface, which mainly shows asperities, which are larger than the microasperities of the flat compacted powder surfaces. This reduces the mechanical influence of the surface structure on the sliding process, and a dynamic friction can occur earlier. The friction force between Salmeterol Xinafoate and lactose particles is higher than the friction force estimated in the particle-on-surface experiments, but the coefficient of friction is much smaller. Furthermore, ploughing appears to be the dominant mechanism in the particle-on-particle experiments, whereas adhesion appears to be the only factor involved in the particle-on-surface experiments. This could be due to the fact that Salmeterol Xinafoate particles are strong artificial agglomerates of fine particles of 1–2 μm. The hard crystalline surface of lactose particles could lead to an abrasion of such primary Salmeterol Xinafoate particles, whereas the surface of compacted lactose is itself weak and could therefore not act as an abrasive. This suggests that surface roughness is an important consideration if the proportion between friction due to the adhesion or ploughing mechanisms has to be evaluated. However, particle-on-surface and particle-on-particle experiments are not equivalent for a further reason. The lactose carrier particles are not rectangular, and the angle between the support surface and the centrifugal force vector, which is adjusted in the experiment, and the angle between a single lactose carrier particle and the centrifugal force vector, which is unknown, may be different. Therefore, particle-on-particle friction experiments do not provide accurate α values. This effects any calculation of friction forces or coefficients of friction. Therefore, particle-on-particle friction experiments should always be accompanied by particle-on-surface experiments, if the mechanisms involved are not to be evaluated.

Particle size fractions LF1 and SFa are comparable in particle size and hence further comparisons can be made between the materials. Erhard [17] related the coefficient of friction between two materials to the reversible energy of adhesion, W_o, which can be calculated as described by Fowkes [32] from the polar and dispersion component of the surface free energy of the materials in contact, or as described by Good [33] from the Lewis acid–base terms of the surface free energies. Such calculations have been reported previously [29] for the materials studied in this paper. Erhard [17] proposed an exponential function, but because the reversible energy of adhesion increases in the order Salmeterol Xinafoate (autoadhesion) < adhesion of Salmeterol Xinafoate on lactose < lactose (autoadhesion), and the coefficient of friction (LF1/SFa) increases in the order Salmeterol Xinafoate (autofriction) < lactose (autofriction) < friction of Salmeterol Xinafoate particles on lactose, Erhard's relationship is not applicable. However, the friction force can be drawn as a function of the reversible energy of adhesion (Fig. 1). The use of the Lewis acid–base terms to calculate W_o leads to a linear relationship between the friction force and the reversible energy of adhesion, whereas the use of Fowkes' equation provides a non-linear graph. The same relationship can be obtained for the adhesion force (Fig. 2). Therefore, both friction and adhesion forces depend on the reversible energy of adhesion, and a prediction on the friction and adhesion force from such parameters might be possible.

Maugis and Pollock [21] found that the ratio between force of adhesion and applied load is proportional to the yield stress of a material, which is 150.1 MPa for lactose [34] and about 19.7 MPa for

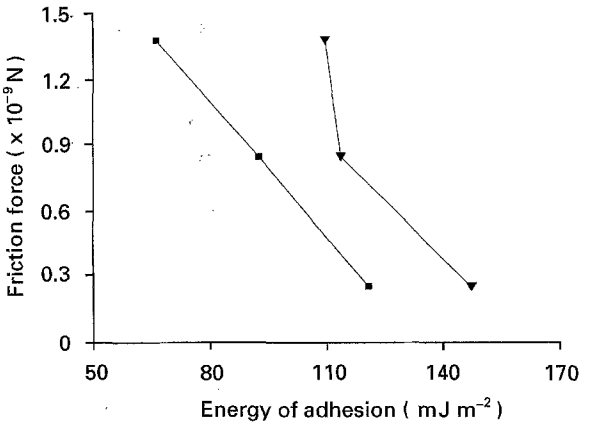

Figure 1 The friction force as a function of the reversible energy of adhesion for SFa–Salmeterol Xinafoate surface, SFa–lactose surface and LF2–lactose surface: (■) reversible energy of adhesion calculated from Lewis acid–base terms of the surface free energies, (▼) reversible energy of adhesion calculated from polar and dispersion components of the surface free energies.

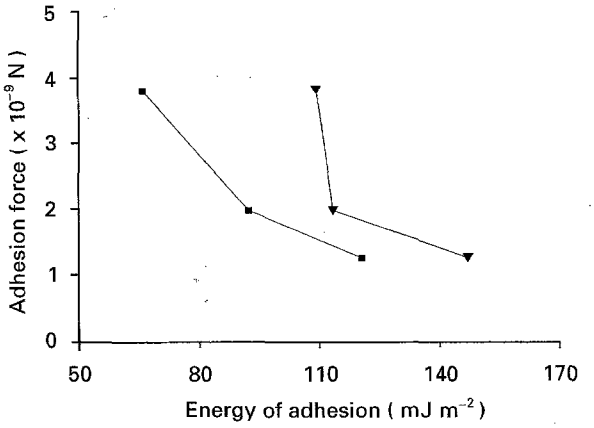

Figure 2 The adhesion force as a function of the reversible energy of adhesion for SFa–Salmeterol Xinafoate surface, SFa–lactose surface and LF2–lactose surface. (■) reversible energy of adhesion calculated from Lewis acid–base terms of the surface free energies, (▼) reversible energy of adhesion calculated from polar and dispersion components of the surface free energies.

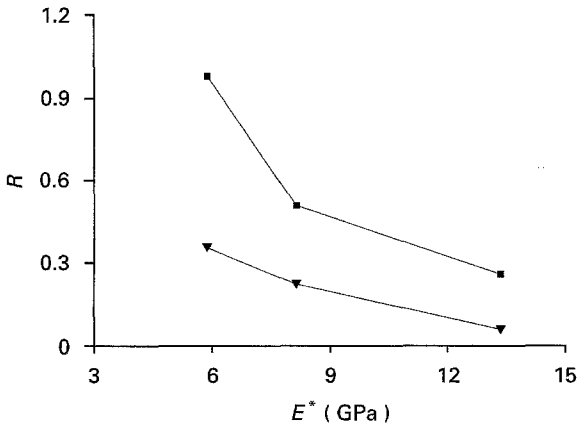

Figure 3 The ratio, R, between force of adhesion and press-on force (■) and the ratio between friction force and press-on force (▼) as a function of the reduced Young's modulus, E^*, of the materials in contact.

Salmeterol Xinafoate (derived from Young's modulus reported in [29]). The ratio between the force of adhesion and the applied load is 0.979 (autoadhesion of Salmeterol Xinafoate), 0.506 (adhesion between Salmeterol Xinafoate and lactose) and 0.255 (autoadhesion of lactose). According to the results of Maugis and Pollock [21] this ratio is small for a material with a low yield stress and approaches one for those with a high yield stress value. The adhesion values are in agreement with this theory, and it appears that the theory can also be applied to the friction forces. The ratios are 0.355, 0.219 and 0.053 for Salmeterol Xinafoate (autofriction), friction of Salmeterol Xinafoate on lactose and lactose (autofriction), respectively.

Adhesion and friction are also related to the elastic properties of a material [14, 31]. Therefore the reduced Young's modulus, E^*, [35] for the contact of two materials has been calculated. The values of E^* are 13.35 GPa (lactose on lactose), 8.14 GPa (lactose on Salmeterol Xinafoate) and 5.85 GPa (Salmeterol Xinafoate on Salmeterol Xinafoate). Fig. 3 shows the ratio of the friction force–press-on force and the ratio of the adhesion force–press-on force as a function of E^*. The ratio based on the friction forces approximates to a linear function of the reduced Young's modulus, whereas the use of the adhesion forces provides a non-linear relationship.

4. Conclusions

The centrifuge technique used in particle adhesion experiments can be modified to allow friction forces of single particles to be measured. Both flat compacted powder surfaces and large single particles can be used as substrate surfaces. In friction tests, particle-on-surface experiments are more accurate than particle-on-particle experiments, and the two methods provide different values for the assessment of friction. The friction angle necessary to transform static friction into dynamic friction depends on the size of the attached particles. The larger the particles, the smaller is the friction angle where first sliding or rolling processes occur. The variability of the detachment forces in friction experiments depends on the nature of the dynamic friction. Rolling friction forces are less variable than sliding friction forces.

Generally, the static coefficient of friction decreases with an increase in particle size. The autofriction force of lactose particles also increases with an increase in particle size, probably due to a larger true area of contact. The friction force of irregular particles of Salmeterol Xinafoate on compacted lactose surfaces is larger than the autofriction force on compacted Salmeterol Xinafoate surfaces. The differences in the surface roughness of the compacted surfaces were identified as one main reason for this phenomenon. Surface roughness also appears to be an important factor, which supports either adhesion or ploughing as the main mechanism of friction. Forces of adhesion and friction are related to the reversible energy of adhesion. This relationship is a linear function, if the reversible energy of adhesion has been determined from the Lewis acid–base terms of the surface free energy of the materials in contact. The ratio between the force of adhesion and the press-on-force applied, as well as the ratio between the friction force and the press-on force applied, are related to the yield stress of the materials and their reduced Young's moduli.

Acknowledgement

The authors are very grateful to Professor D. Tabor for the advice and discussion of the work.

References

1. R. L. CARR, *Chem. Eng.* **18** (1965) 163.
2. S. B. TAN and J. M. NEWTON, *Int. J. Pharm.* **64** (1990) 227.
3. K. D. ERTEL and J. T. CARSTENSEN, *J. Pharm. Sci.* **77** (1988) 625.
4. M. B. JAMES and J. M. NEWTON, *Powder Technol.* **34** (1983) 29.
5. A. D. ZIMON, "Adhesion of Dust and Powder", 2nd Edn. (Consultants Bureau, New York, 1982) pp. 24–29.
6. A. KHILNANI, in "Particles on Surfaces I", edited by K. L. Mittal (Plenum Press, New York, 1988) pp. 17–35.
7. F. PODCZECK, J. M. NEWTON and M. B. JAMES, *Powder Technol.* **83** (1995) 201.
8. G. BÖHME, H. KRUPP, M. RABENHORST and G. SANDSTEDE, *Trans. Int. Chem. Eng.* **40** (1962) 252.
9. K. K. LAM and J. M. NEWTON, *Powder Technol.* **65** (1991) 167.
10. F. P. BOWDEN and D. TABOR, "The friction and Lubrication of Solids", Part I, (Clarendon Press, Oxford, 1964) pp. 17–18.
11. N. P. SUH, *Wear* **25** (1973) 111.
12. *Idem, ibid.* **44** (1977) 1.
13. N. P. SUH and H. C. SIN, *ibid.* **69** (1981) 91.
14. J. A. GREENWOOD and K. L. JOHNSON, *Phil. Mag.* **A43** (1981) 697.
15. R. G. HORN, J. N. ISRAELACHVILLI and F. PRIBAC, *J. Colloid Interface Sci.* **115** (1987) 480.
16. M. B. JAMES and J. M. NEWTON, *J. Mater. Sci.* **20** (1985) 1333.
17. G. ERHARD, *Wear* **84** (1983) 167.
18. L. LAVIELLE, *ibid.* **151** (1991) 63.
19. S. K. R. CHOWDHURY and P. GHOSH, *ibid.* **174** (1994) 9.
20. D. MAUGIS, G. DESALOS-ANDARELLI, A. HEURTEL and R. COURTEL, *ASLE Trans.* **21** (1976) 1.
21. D. MAUGIS and H. M. POLLOCK, *Acta Metall.* **32** (1984) 1323.

22. I. M. HUTCHINGS, *Powder Technol.* **76** (1993) 3.
23. H. YOSHIZAWA, Y.-L. CHEN and J. ISRAELACHIVILI, *J. Phys. Chem.* **97** (1993) 4128.
24. S. A. KARPE, *ASLE Trans.* **25** (1981) 537.
25. S. T. SPURR, *Wear* **79** (1982) 301.
26. S. BHATTACHARYA and K. L. MITTAL, *Surf. Technol.* **7** (1978) 413.
27. A. E. HAWKINS, "The Shape of Powder-Particle Outlines" (Research Studies Press, Taunton, 1993) p. 46.
28. F. PODCZECK, J. M. NEWTON and M. B. JAMES, *J. Adhesion Sci. Technol.* **8** (1994) 1459.
29. *Idem, ibid.* **9** (1995) 475.
30. B. N. J. PERSSON, *J. Electron Spectrosc. & Related Phenomena* **64/65** (1993) 403.
31. A. M. STONEHAM, M. M. D. RAMOS and A. P. SUTTON, *Phil. Mag.* **A67** (1993) 797.
32. F. M. FOWKES, *Ind. Chem. Eng.* **56** (1964) 40.
33. R. J. GOOD, *J. Adhesion Sci. Technol.* **6** (1992) 1269.
34. R. J. ROBERTS and R. C. ROWE, *Int. J. Pharm.* **36** (1987) 205.
35. S. P. TIMOSHENKO and J. N. GOODIER, "Theory of Elasticity", 3rd Edn (McGraw Hill, Singapore, 1970) pp. 409–422.

Received 23 September 1994
and accepted 24 May 1995